

# Production of a Narrow Magnetized Plasma by a High Temperature Cathode

Shinsuke IMAKITA, Toshiro KASUYA, Naoki MIYAMOTO<sup>1)</sup>,  
Satoshi SHIMAMOTO, and Motoi WADA

*Graduate School of Engineering, Doshisha University, Kyotanabe, Kyoto 610-0361, Japan*

<sup>1)</sup>*Nissin Ion Equipment Co. Ltd, Minami-ku, Kyoto, 610-0332, Japan*

(Received: 2 September 2008 / Accepted: 4 November 2008)

Electric current that heats a high temperature cathode of a Bernas ion source deforms the shape of an ion source plasma confined in an external straight magnetic field. We have developed a co-axial cathode to reduce the plasma deformation due to the cathode heating current. The cathode was mounted to a Bernas ion source to see the advantage over a commonly employed hair-pin shaped high temperature filament cathode operated with a similar magnitude of heating current. Precise measurement of ion current distribution by a Langmuir probe showed that the plasma produced by a hair-pin cathode largely shifts toward the negative end of the filament. The plasma produced by the co-axial cathode has shown a little shift caused by a bent of the external magnetic field itself. An electron density of the plasma produced with the co-axial cathode is nearly an order of magnitude greater than that produced with a hair-pin filament.

Keywords: ion source, high temperature cathode, magnetic field, ion production efficiency.

## 1. Introduction

Present day ion implanters for semi-conductor industries require a longer operating life and higher gas efficiency. A high temperature cathode adapted to a Bernas ion source produces a source plasma in wide range of discharge power with elongated operation time [1]. Several modifications in the cathode structure had been attempted to improve the ion source performance. For example, indirectly heated cathode (IHC) has a thick refractory metal plate durable against plasma heating for prolonging the operation life [2]. However, an IHC ion source needs a complicated power supply system, and extra components to assemble the source. On the other hand, a power supply system for a directly heated high temperature cathode is much simpler than those for other high temperature cathodes like the one for an IHC. Thus, many researchers had studied to extend life times of directly heated cathodes [3].

Ehlers and Leung had investigated the electron emission from filament cathodes in gas discharge [4]. They showed that the discharge current had concentrated to the area of the cathode biased most negatively, and the highest temperature appeared near the area. They also had pointed out the magnetic field produced from the filament heating current affected the trajectories of electrons emitted from the filament. The heating current can cause even worse concentration of heat load under the presence of an external magnetic field for plasma confinement, as the magnetic field produced by the heating current couples to the confinement magnetic field. Thus, we designed a co-axial cathode which produces no magnetic field with a heating current

to investigate if the structure is effective in reducing inhomogeneity of electron emission arising from the coupling between the cathode heating current and the confinement magnetic field. The performance of the cathode was compared with a hair-pin shaped filament cathode, which is commonly used for Bernas ion source.

## 2. Experimental setups

### 2-1. Co-axial cathode

A high temperature cathode having a co-axial electrical current carrying path for heating is fabricated with the structure adaptive to the Nissin's BEAR (Bernas-type Electron Active Reflection) ion source [5]. Schematic illustration of a co-axial cathode is shown in Fig.1. The cathode consists of a tungsten centre wire of 2 mm diameter, and a tantalum tube of 5 mm outer diameter and 4.8 mm inner diameter.

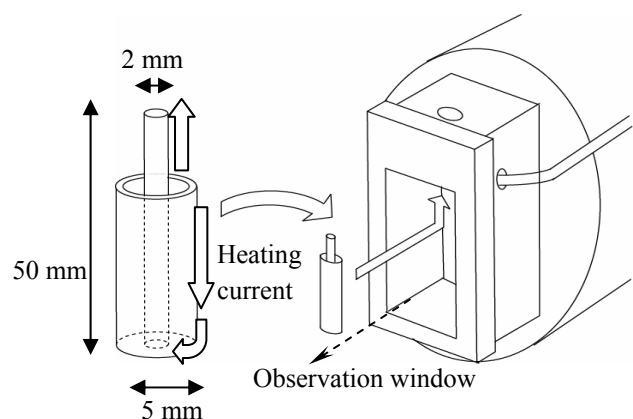


Fig.1 Schematic illustration of a co-axial cathode and the experimental setup.

author's e-mail: mwada@mail.doshisha.ac.jp

No magnetic field is produced around the outer surface of the cathode except at the top end where the cathode directly contacts to the plasma. The magnetic field produced near the top end is axially symmetric, and no inhomogeneous interaction between the field produced by the cathode heating current and the external magnetic field is present. The hair-pin filament used for making a comparison with the coaxial cathode is 2 mm diameter having a 15.0 mm radius of curvature at the top.

**2-2. Ion source and test chamber**

The experimental apparatus is shown in Fig. 2. The arc chamber is mounted at the top of an ion source supporting structure. By applying a 150 A heating current to a co-axial cathode, about 0.45 A discharge current is obtained with -60 V discharge voltage. Outside of the test chamber is mounted an electromagnet with the iron yoke to produce a linear magnetic field for the plasma confinement. A viewing port is attached at the opposite side of the ion source mounting flange, so that plasma produced in the arc chamber can be observed from the front side of the ion source through a viewing window.

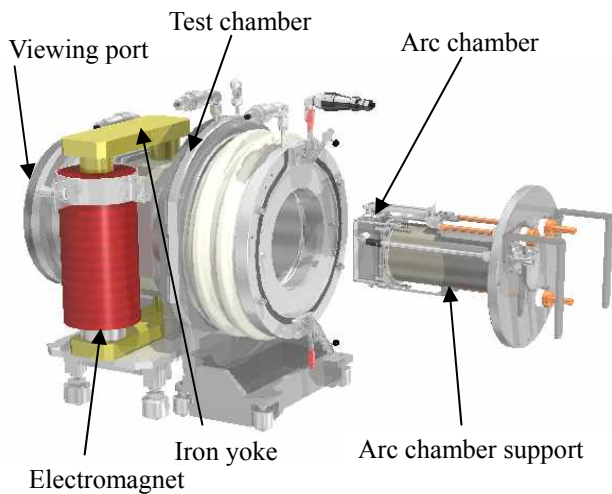


Fig.2 Schematic diagram of the test ion source.

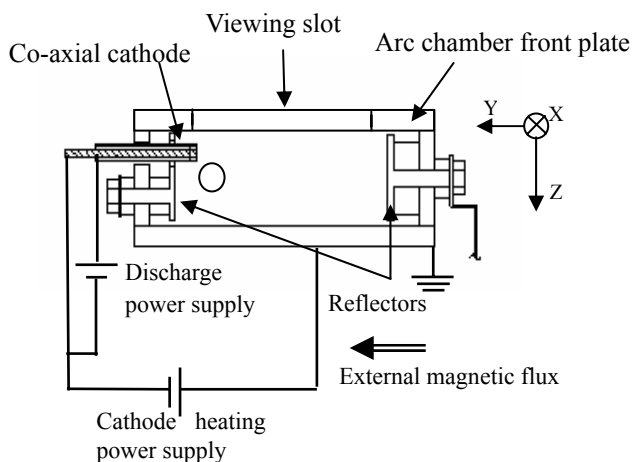


Fig.3 A cross-sectional view of the arc chamber.

Figure 3 shows a cross-sectional view of the arc chamber. The arc chamber is made of carbon to reduce reflected light from the tungsten filament to make the observation of light emission from the source plasma easier. Two reflectors are mounted to enhance ionization efficiency of the ion source. Axis directions in Langmuir probe measurements are assigned as shown in Fig. 3.

**3. Results and discussion**

**3-1. Temperature distribution**

Pictures of the cathodes were taken by an infrared camera (IR) by running about 60 A of heater current. The IR images of the cathode surfaces are shown in Fig. 4. In the case of a hair-pin cathode, inhomogeneous intensity distribution corresponding to inhomogeneity in temperature distribution is observed. On the other hand, co-axial cathode exhibited a homogeneous IR emission over the entire exposed area. The homogeneous temperature distribution should realize homogeneous electron emission from the entire cathode area, which should result in suppression of local heating.

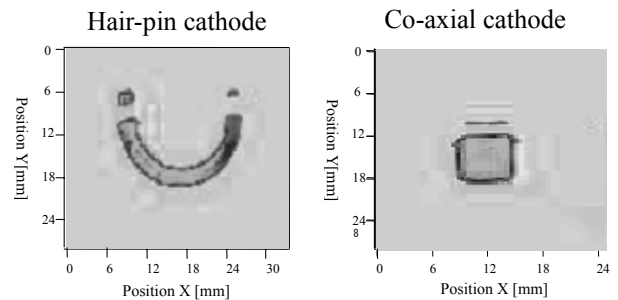


Fig.4 Distributions of infrared radiations measured by an IR camera.

**3-2. Discharge characteristics**

The pictures of source plasmas produced by both cathodes were taken through a 488 nm optical interference filter with an experimental setup shown in Fig. 5. Plasmas were maintained with 0.45 A discharge current at 0.6 Pa Argon gas pressure. The co-axial cathode needed a heating current 10 A larger than the current to heat up the hair-pin filament to obtain this discharge current. The co-axial cathode has larger surface area than the hair-pin filament and the radiation cooling requires more heating power.

The lower panel of Fig. 5 shows a light intensity distribution of source plasma along the analysis line drawn in the figure, which is the center of the arc chamber. In the case of a hair-pin filament, the source plasma shifted to the negative end of the filament by 5 to 7 mm, when the direction of heating current was changed. On the other hand, this shift of source plasma was not observed for the co-axial cathode.

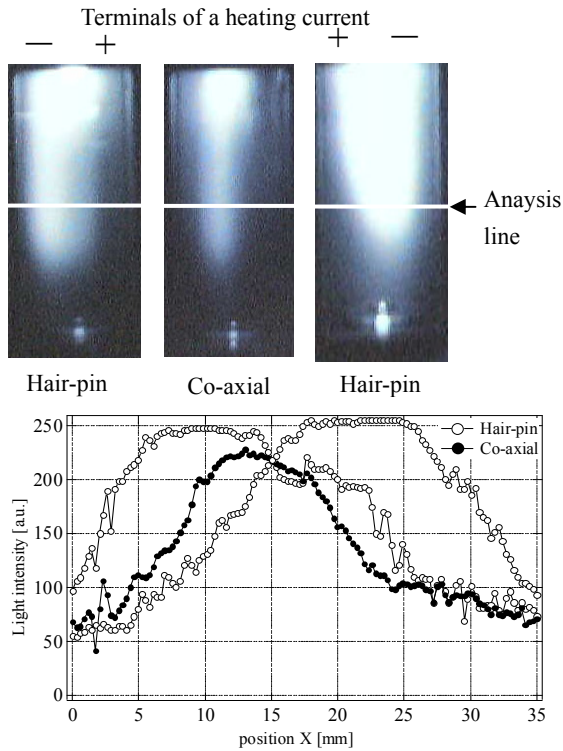


Fig.5 Light intensity distributions of source plasmas.

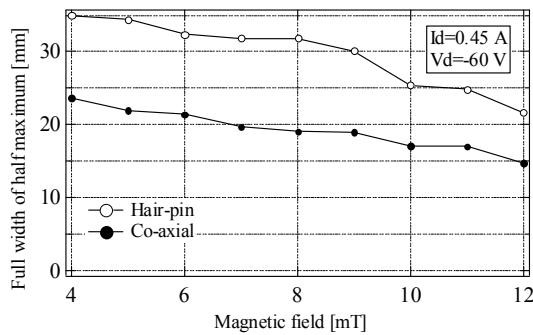


Fig.6 Full widths at half maximum of the light intensity distributions of source plasmas plotted as functions of magnetic field strength.

In addition to not showing any shift of the plasma, radius of the source plasma produced by the co-axial cathode was found narrower than that of a hair-pin cathode. Therefore, the efficiency of ion beam extraction should increase with the concentrated plasma shape. The reason for observing a small shift for plasma produced by a co-axial cathode is the bending of the external magnetic field due to an asymmetric arrangement of the electromagnet.

Full widths at half maxima in the light intensity distributions are plotted as functions of magnetic field intensity in Fig. 6. The width of the source plasma became narrower as external magnetic field increased for both cathodes. The widths of light intensity of the source plasma produced by a co-axial cathode do not exceeded those by a hair-pin cathode. These result shows a co-axial cathode can produce narrower source plasmas than a

hair-pin cathode.

The spatial distributions of electron density were measured by moving a Langmuir-probe in X, Y, and Z directions as shown in Fig. 7. Discharge conditions were adjusted to 60 V/0.25 A discharge power, 0.6 Pa Argon gas pressure, and 6 mT external magnetic field for both cathodes. The results of X profiles are shown in Fig. 8 for Y=0 and Z=7 mm. In the case of hair-pin filament, electron density distribution is broad in X direction, while it is more focused to the center of the chamber in the case of the co-axial cathode. In addition, co-axial cathode produced an electron density as high as ten times that produced by a hair-pin cathode.

Corresponding to Fig. 5, Fig. 8 shows the source plasma produced by the hair-pin filament has a peak shifted toward the direction of negative X, because of plasma concentration to the negative terminal of the heating current. Meanwhile, a plateau region of electron density as wide as 5 mm was observed for the co-axial cathode,

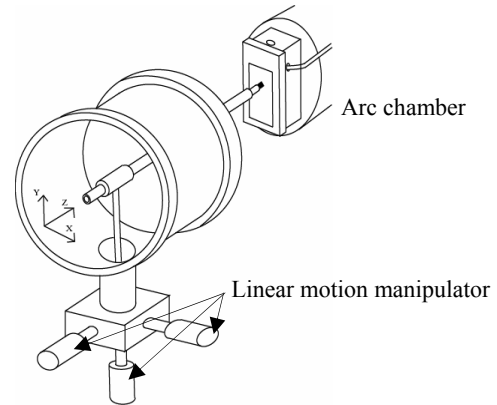


Fig.7 Illustration of probe manipulator system.

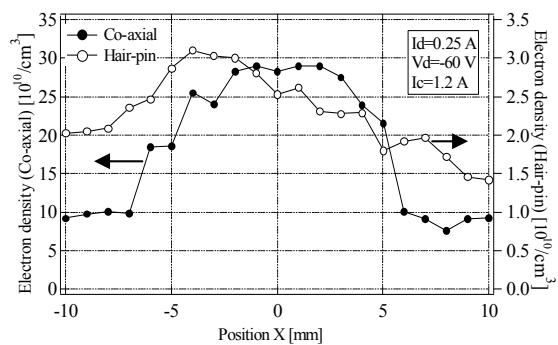


Fig.8 Electron density distributions along the X direction.

The electron density distribution plotted along the Z-direction is shown in Fig. 9. The peak in the electron density distribution of a plasma produced by the co-axial cathode was higher than that produced by the hair-pin cathode. In the case of the co-axial cathode, a peak of electron density was observed at the point Z=7 mm, corresponding to the point right under the cathode as shown in Fig. 9. The electron density distribution for the

plasma produced by the hair-pin cathode was quite homogeneous in Z direction. Namely, the plasma produced by a hair-pin cathode nearly fills the entire region inside the arc chamber.

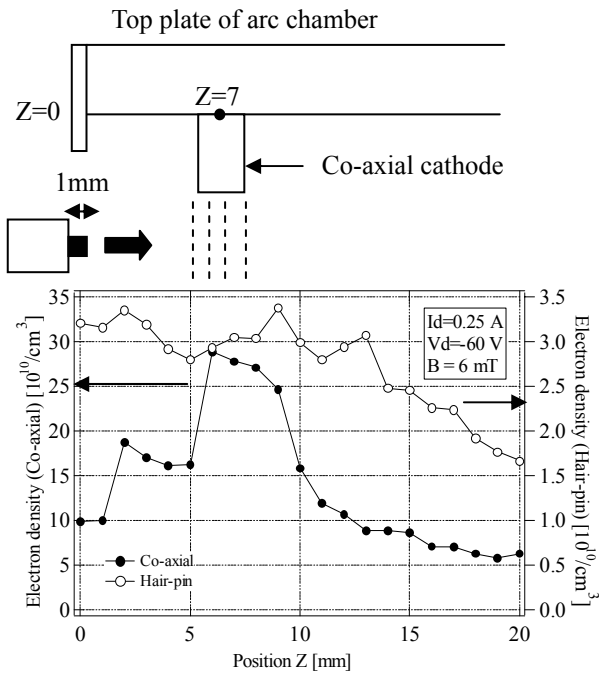


Fig.9 Electron density distribution along the Z direction.

From the above results the plasma produced by a co-axial cathode is much more concentrated at the center than plasma produced by the hair-pin cathode in both X and Z directions. The steep gradient in the Z direction near the plasma boundary will enhance diffusion of plasma toward the extraction hole of the ion source to enlarge the ion beam current.

To further investigate the distribution of electron density, we measured 2-dimensional distributions of saturated ion current at X-Z plane. The results are shown in Fig. 10. In the case of the co-axial cathode, a peak is observed at point Z=7 mm again. On the other hand the peak for the plasma produced by the hair-pin cathode shifted to point Z=0 mm, probably due to the influence of the magnetic field produced by the heating current. Both cathodes exhibits a tendency of higher ion saturation current toward the side of negative X due to bending of the external magnetic field.

#### 4. Summary

At the ion extraction area of the Bernas ion source, the co-axial cathode produces narrow and dense plasma in a weak magnetic field. Meanwhile the shift and broadening of the plasma was caused by a coupling between a linear confinement magnetic field and the field produced by heater current running through the hair-pin filament cathode. Although the co-axial cathode needs a

heating current higher than the hair-pin cathode to obtain the same discharge current, the efficiency in producing ion beam for a fixed arc power is higher. In fact, the ion beam current as much as twice of that produced by a hair-pin cathode was obtained from the ion source equipped with a co-axial cathode [6].

#### Acknowledgments

The authors thank Y. Konishi and S. Soda at Doshisha University for their technical assistance on the experiment. Valuable cooperation for realizing the co-axial cathode production from Y. Minosaki and H. Sasaoka of Creative Technology Corporation are greatly acknowledged.

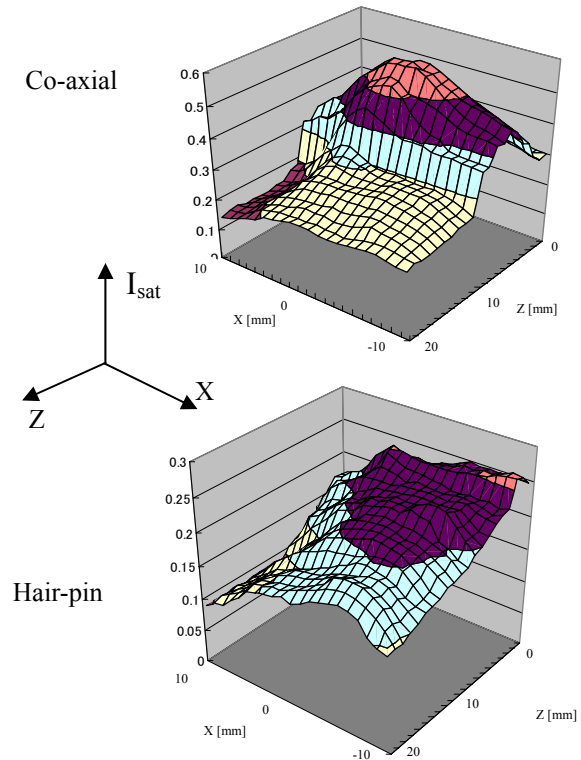


Fig.10 Two dimensional distributions of ion saturation current.

- [1] T. V. Kulevoy, R. P. Kuibeda, S. V. Petrenko, V. A. Batalin, V. I. Pershin, and G. N. Kropachev, *Rev. Sci. Instrum.* **77**, 03c110 (2006).
- [2] K. Tanaka, S. Umisedo, K. Miyabayashi, H. Fujita, T. Kinoyama, N. Hamamoto, T. Yamashita and M. Tanjyo, *Proceedings of 16th International Conference on Ion Implantation Technology*, 421 (2006).
- [3] S. R. Walther, *Rev. Sci. Instrum.* **65**, 1307 (1994).
- [4] K. W. Ehlers and K. N. Leung, *Rev. Sci. Instrum.* **50**, 356 (1979).
- [5] N. Miyamoto, K. Miyabayashi, T. Yamashita and H. Fujisawa, *Rev. Sci. Instrum.* **73**, 819 (2003).
- [6] N. Miyamoto, N. Hamamoto, S. Imakita, A. G. Mendenilla and M. Wada, to appear in *Proceedings of 17th International Conference on Ion Implantation Technology* (2008).